Decay of the 4*d* hole states of Xe studied by photoelectron-photoelectron coincidence spectroscopy

K. Okuyama, J. H. D. Eland,* and K. Kimura
Institute for Molecular Science (IMS), Okazaki 444, Japan
(Received 20 December 1989)

The formation of Xe^{2+} by decay of 4*d* hole states in xenon has been investigated by observing both the $N_{4,5}OO$ normal Auger spectra and the resonantly excited spectra using synchrotron radiation and a new form of electron–electron coincidence spectroscopy involving a magnetic-bottle time-of-flight analyzer. Direct double Auger processes from the resonance populate all accessible states of Xe^{2+} while indirect processes via superexcited Xe^{+} levels populate ground and lower excited states of Xe^{2+} preferentially.

INTRODUCTION

When a 4*d* hole is created in atomic xenon, either with complete removal of the electron or with its excitation to a normally vacant orbital, the excited atom relaxes mainly by electron reorganization leading to further electron ejection. The decay processes have been studied both by electron spectroscopy[1–7] and by measurements of the yield of Xe^{+}, Xe^{2+}, and Xe^{3+} ions as functions of incident photon energy.[8,9] The much weaker competing process of fluorescence to the Xe^{+} ground states has also been studied[10] and shows that the hole states have intrinsic widths of 0.14(4) eV. As a result of all this work, we know that Xe^{+} $4d^{9}5s^{2}5p^{6}\,^{2}D$ decays mainly ($\sim 80\%$) to Xe^{2+}, populating states of both the simple configurations $5s^{2}5p^{4}$, $5s5p^{5}$, and $5s^{0}5p^{6}$ and also states from configurations such as $5s^{2}5p^{3}5d$. Many details of the branching ratios to the individual states can be understood theoretically with the help of relativistic multiconfiguration calculations.[1,11] The competing decay to Xe^{3+} by two-electron ejection is much less well characterized, but a direct process, rather than autoionization via excited levels of Xe^{2+}, has been suggested on the basis of ion yield measurement.[9]

Decay of the pre-edge resonances of neutral Xe, such as $4d^{9}5s^{2}5p^{4}6p$, provides a rich spectrum of final states, partly because the initially excited electron can be either a participant or a spectator in the process. In the best-studied case the relative yields of Xe^{+}, Xe^{2+}, and Xe^{3+} from the $4d^{9}5s^{2}5p^{6}(^{2}D_{5/2})6p$ resonance at 65.1 eV (with continuum subtracted) are 13%, 86%, and 0.5% respectively, while the yield of stable neutral Xe by fluorescence, which can be estimated by comparing the absolute absorption and ionization cross sections, is unknown ($\sim 10\pm 15\%$), but certainly small. On the basis of the electron and ion spectra, many authors have deduced that one major process forming Xe^{2+} is autoionization via excited states of Xe^{+} ("resonant spectator satellite enhanced" double ionization), while Becker *et al.*[2] have emphasized the existence of more direct processes giving a continuous electron spectrum (variously called "resonant shakeoff" or "resonant double Auger"). The final-state distribution of Xe^{2+} produced by these decay routes is unknown, however, as only single-electron spectra have been available hitherto.

Both the Auger effect and the resonant Auger effect involve the emission of two electrons within a very short period. Such processes can be fully characterized only if both electrons are energy analyzed and detected in coincidence, since clear characterizations of both the final state (from the sum of the electron energies) and any intermediate states (from single-electron energies contributing to a given sum) are then possible. Investigations of double ionization of Ar, Xe, and small molecules[12,13] below inner-shell thresholds and of solid Xe (Ref. 14) by this photoelectron–photoelectron coincidence (PEPECO) technique have been reported recently. We here report a PEPECO study of the xenon inner-shell ionization, using a new apparatus installed at the synchrotron radiation source, Ultraviolet Synchrotron Orbital Radiation Facility (UVSOR), at the Institute for Molecular Science (IMS). The essence of the technique is to record times of flight of electrons in two opposed directions, referenced to the time of synchrotron radiation pulses. The electrons are detected in coincidence, and as the whole spectrum is accessible for each electron at all times, complete two-parameter spectra of intensity as a function of two-electron energies are built up.

Because the resolution of the prototype instrument is still poor for technical reasons, the present paper is an introduction to the new technique and a preliminary report on the dynamics of 4*d* hole decay in Xe atomic species.

EXPERIMENTAL APPARATUS AND TECHNIQUE

The experiment was mounted on line 3A2 of UVSOR, and for reasons of intensity it used light from the 25-pole undulator,[15] selected by a grazing incidence monochromator.[16] For each wavelength the undulator gap was set to provide light in a strong (usually odd) harmonic, and the monochromator was then used to select within the undulator bandwidth. This arrangement gave about 200 times more intensity than use of the monochromator with a simple bending magnet, an increase which was essential

to overcome the light loss associated with restricting the beam to a pencil ray of 1-mm^2 cross section. Tight collimation was effected by a series of small sharp-edged apertures to ensure that no light could hit metal surfaces near the ionization volume of the electron energy analyzer and that the ionization volume, defined by the intersection of the light with an effusive gas jet, was approximately 1 mm^3 in size.

Energy analysis was done using a commerical version of the magnetic-bottle analyzer designed by Kruit and Read,[17] with a second electron detector added in the arm opposite to the main flight path (Fig. 1). A small ($\phi = 18$ mm) multichannel plate detector[18] was mounted within the tubulation leading to the pole piece, providing an electron flight path of 4 cm, to be contrasted with the 50-cm path length of the main flight tube. This type of arrangement is essential in order to implement a novel scheme of using storage ring radiation pulsed with a high repetition rate to measure electron flight times that may greatly exceed the interpulse spacing (here, 178 ns). When two electrons are emitted, as in double photoionization, an observable event is one in which one electron impinges on each detector. Since one arm is much shorter than the other, the short flight-path electron will arrive at its detector before the other for the overwhelming majority (greater than 99%) of partitions of the total available energy between the two electrons. The additional flight time of the second electron, after the arrival of the first one, can be measured unambiguously, irrespective of the number of pulse periods it covers. For the first electron, the short flight path also means that a large change in deduced electron energy is implied by a change of one pulse period in the flight time; the absolute flight time can almost always be determined correctly on the assumption that it is less than one interpulse period (less than 178 ns, corresponding to 0.14 eV), unless energy conservation dictates the addition of a single full period to the apparent flight time. For our geometry this strategy gives correct absolute flight times for more than 99% of energy partitions between two electrons sharing a total of 10 eV and for 96% of pairs sharing 1 eV. At lower total energies an increasing proportion of two-electron events may be incorrectly interpreted.

Contamination of the light by passage of higher orders through the monochromator from high undulator harmonics proved troublesome in the early states of the experiment, but once recognized it could be minimized by judicious choice of the undulator harmonic for each wavelength.

The electron analyzers were calibrated using the well-known single-electron photoelectron peaks of neon and xenon taken at a variety of wavelengths. No retarding fields were used in either flight path. For the long analyzers electron flight times were precisely linear in $E^{-1/2}$, as expected, and the energy resolution (15 meV at 2 eV claimed by the manufacturers) was limited entirely by the photon bandwidth of about 200 meV (1.6 Å at 300 Å). The short analyzer flight times were shorter than expected at low energies, a deviation that we attribute to field penetration from the channel plate electron multiplier potential. The flight times (T) could be well fitted by a two-term expression of the form

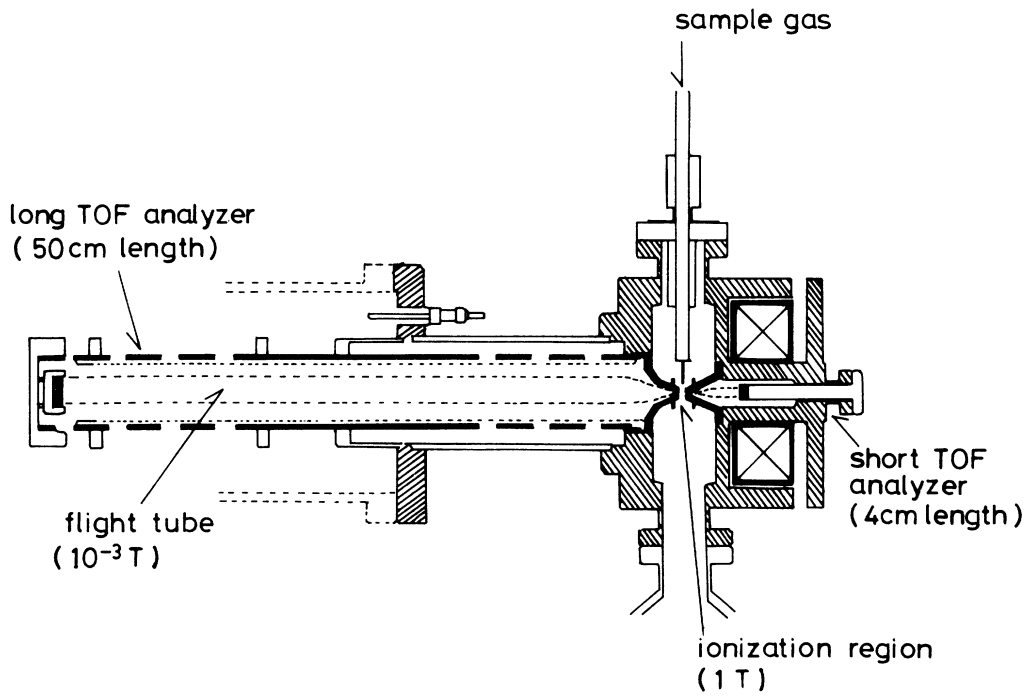

FIG. 1. Schematic diagram of the apparatus. External high permeability shields are used to eliminate the geomagnetic field and stray fields from the bending magnets of the storage ring.

$$\mathcal{T} = AE^{-1/2} - BE^{-1} .$$

The resolution of the short analyzer was limited at low electron energies by broad asymmetric tails on the long-flight-time sides of peaks, possibly because the detector was situated within the region of divergent electron trajectories. At higher electron energies the resolution was limited by the ±1-ns time resolution of the electronic system. As a result, the actual peak width was about 1.5 eV for electron energies below 10 eV, deteriorating to about 5 eV for electrons of 40 eV energy. This poor resolution constitutes the major limitation of the current instrument performance.

The electronic system used fast amplifiers (EG&G, FTA420A) and discriminators (EG&G, 934) followed by an eightfold 1-ns resolution multihit time-to-digital converter (TDC, LeCroy 7208) read out through a CAMAC interface (cc/9800-FSI) into a microcomputer (NEC PC-9801 UX). For electron-electron coincidence work the TDC was started by an electron signal from the short analyzer and recorded stop signals from both the next UVSOR pulse and any electron signal from the long analyzer. A home-built external logic unit caused the TDC to be reset, with no computer readout, if a second electron signal was not present. Accessibility of computer memory limited the amount of data actually recorded in each experiment to intensities in cells of a 100×100 array, one dimension representing flight times on the short energy analyzer with 1-ns bins, while the other accumulated long analyzer flight times up to 1000 ns with 10-ns bins. This binning artificially degraded the resolution of the long analyzer data, but still left it better at all energies than that of the short analyzer.

RESULTS

Auger effect

The raw experimental results consist of small numbers of counts in each element of a 100×100 array, representing the two-parameter electron-electron coincidence spectrum. If wavelengths shorter than 183.6 Å are present, even as second-order contamination of the light, the spectra are dominated by the Auger effect: a spectrum taken at 167 Å (74.1 eV) is shown in Fig. 2. The major feature is the double cross, made up of the Auger electron spectra recorded in each analyzer after detection in the other analyzer of the electron ejected in forming a $^2D_{5/2}$ or $^2D_{3/2}$ state of Xe^+. Individual counts outside the cross, spread apparently haphazardly over the rest of the spectrum, are not noise, but show the presence of triple ionization and a small contribution from "direct" double-ionization processes producing electron pairs with a continuous distribution of energy. By selecting a vertical or horizontal strip of the two-parameter spectrum, we can derive the Auger spectrum for either the $^2D_{5/2}$ or for the $^2D_{5/2}$ hole state: a spectrum for $^2D_{5/2}$ is shown in Fig. 3. The major features of the well-known Auger spectrum are clearly visible, though unresolved, and a rather weak peak at 2 eV electron energy also emerges. The relative intensities of the Auger lines corresponding to the

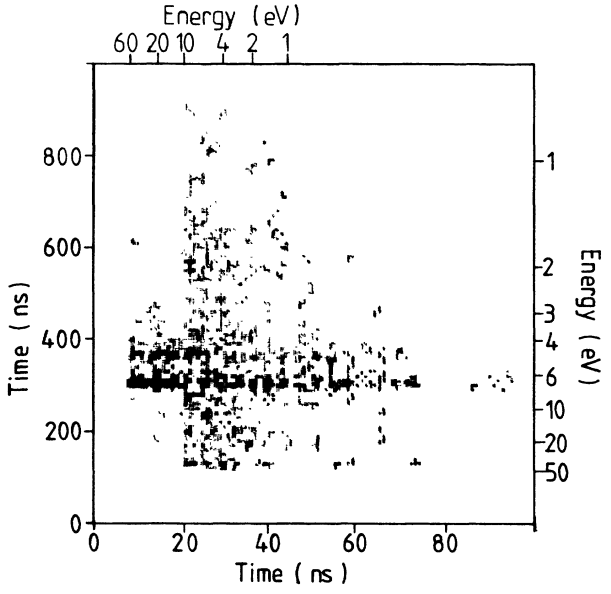

FIG. 2. PEPECO spectrum of xenon at 167 Å (74.1 eV) with intensities coded as dot density. Times of flight in the short and long analyzers (horizontal and vertical axes, respectively) are on a linear scale, as measured.

Xe^{2+} configurations $5s^25p^4$, $5s5p^5$, $5s^25p^3np$ or $5s^25p^3nd$, and $5s^05p^6$ are in the apparent ratios 2:1:1:1, in fair agreement with previous work.

The weak peak at ~2 eV electron energy is a new observation; it is found in our PEPECO spectra at all wavelengths short enough to populate ^2D and is possibly visible in previous Auger electron spectra,[1,2] where it could not, however, be distinguished from other sources of low-energy electrons. To appear in the PEPECO spectrum it must be a two- (or more) electron ejection, and the spectra show that it is clearly associated with the $4d_{5/2}$ hole. It most probably represents triple ionization to the ground configuration $5s^25p^3$ of Xe^{3+} [threshold 64.1±0.3 (Refs. 9 and 19)], for which 3.4 eV energy is

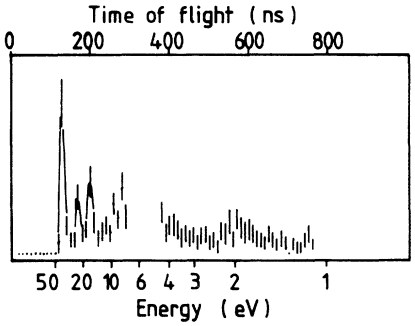

FIG. 3. Auger spectrum of Xe^+ $^2D_{5/2}$ at 167 Å derived from a vertical strip of Fig. 2 around an electron energy of 6.6 eV in the short analyzer. A gap has been left where the horizontal Auger spectrum of Fig. 2 interferes, and solid lines have been drawn to guide the eye between the experimental error bars in the high-energy region.

available at the $^2D_{5/2}$ hole-state energy. Even if the initial step is production of a state of Xe^{2+} at about 65.5 eV, such a state would certainly autoionize to Xe^{3+} afterwards. The third electron would be ejected with 1.4±0.3 eV energy, and peaks in the full PEPECO spectrum should appear at energies (in eV) (6.6, 2.0) (observed), (6.6, 1.4), and (2.0, 1.4). The predicted peaks involving 1.4-eV electrons are unfortunately not convincingly seen in our spectra because of poor statistics, but the possibility of searching for them and thereby clarifying the triple-ionization mechanism exemplifies the power of the PEPECO technique.

Resonant Auger effect at 65.1 eV

By careful choice of undulator harmonic, we were able to obtain 65.1 eV radiation almost free from second-order contamination and thereby to record a spectrum, illustrated in Fig. 4, at the peak of the $4d^9 5s^2 5p^6 6p(^1P)$ resonance of neutral Xe. This PEPECO spectrum shows Xe^{2+} formation exclusively: Xe^+ cannot appear, and Xe^{3+} formation is of negligible intensity at this wavelength, as demonstrated by the ion branching ratios. The time-of-flight spectrum is dominated by a hyperbolic ridge crowned by at least two peaks, which corresponds to formation of Xe^{2+} in its ground configuration $5s^2 5p^4$: this ridge, where the total electron energy is ~30 eV is evidently confined to a region where the individual electron energies are greater than some 3 eV. The outer parts of a second ridge, with total energy around 10 eV, are also visible and evidently extend to lower energies of each electron.

The complete PEPECO data in Fig. 4 can be

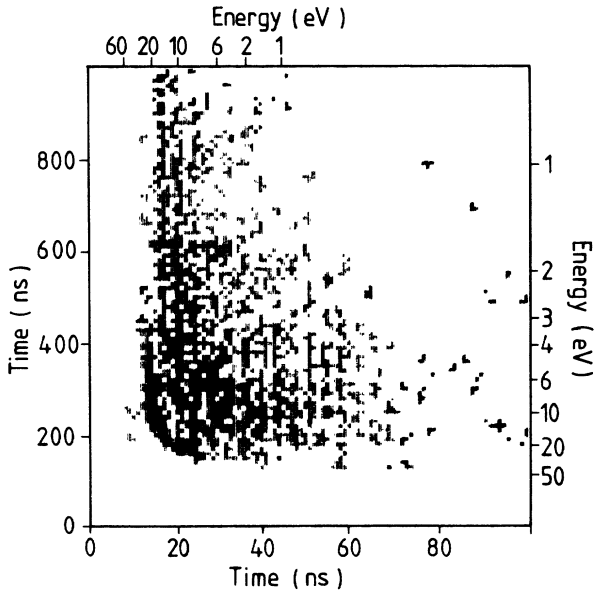

FIG. 4. PEPECO spectrum of xenon at 190.4 Å (65.1 eV) on the peak of the $4d^9 5s^2 5p^6 6p$ resonance, with scales as in Fig. 2. Single isolated counts have been suppressed to improve contrast for display.

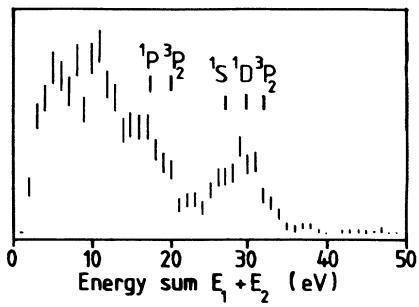

FIG. 5. Spectrum of the energy sum E_1+E_2 derived from the 190.4 Å PEPECO spectrum in Fig. 4, showing data as error bars two standard deviations long. The positions of some final states of Xe^{2+} are indicated.

transformed into several sorts of selective single-parameter spectra. Figure 5 shows the spectrum of total intensity as a function of the sum of the two-electron energies, E_1+E_2. Although the resolution is very poor, four main groups of electron pairs are distinguishable. The highest energy pairs form a broad peak around 30 eV total electron energy, corresponding to formation of Xe^{2+} in its $5s^2 5p^4 \ldots$ ^3P, ^1D, and ^1S states. The ^1D component seems to be strongest (as in the normal Auger) and the other states appear as shoulders. Next there is a broad shoulder at around 16 eV pair energy, a peak at 11 eV pair energy and a final shoulder at about 5 eV pair energy. These three features correspond roughly to three classes of final state, those mainly based on the $5s5p^5$ configuration (16-eV pairs), those based on $5s^2 5p^3 \ldots nl$ configurations (11-eV pairs), and the $5s^0 5p^6$ configuration (5-eV pairs). Within the first two of these groups, there are many individual states which are not resolved; partial resolution is possible by restricting the range of times of flight in the short analyzer to those giving the best resolution, but this seriously distorts the whole pattern.

The relative areas of the four groups in Fig. 5 provide an estimate of the branching ratios to the four final-state configurations of Xe^{2+} as 1:1:2:2 (in order from the ground state of Xe^{2+}), showing more emphasis on high-energy states of Xe^{2+} than in the normal Auger effect.

Figure 6 shows four spectra of a new kind: these are single-electron spectra (using the long time-of-flight analyzer) of electrons forming pairs with total energies in the ranges of each of the four groups seen in the overall E_1+E_2 spectrum (Fig. 5). These are constant-final-state spectra, corresponding to measuring along the ridges in the PEPECO spectra; they show whether a given final state is reached directly (continuum) or indirectly (peaks). Any indirect process via an intermediate Xe^+ state should give two peaks in such spectra, one energy E_1 for formation of Xe^+ from the initial neutral Xe resonance and a second energy E_2 for formation of the final Xe^{2+} state from the Xe^+ intermediate. These two energies also provide two peaks, (E_1, E_2) and (E_2, E_1), symmetrical about the diagonal in the full PEPECO spectrum (Fig. 4). Pairs of peaks are definitely seen in the first two spectra of Fig. 6: the ground state Xe^{2+} complex is clearly

formed via at least one Xe^+ resonance, as are also some states from the $5s5p^5$ configuration. The two peaks that are seen in Fig. 6(a) are centered at electron energies of 21 ± 3 and 9.5 ± 1.5 eV. These might possibly be compatible with the two highest amplitude peaks, at 24 eV and 13 eV, in the 65.1-eV resonance Auger spectra[1-7] but the error is rather large. A much better fit is with the group of peaks in the same spectra around 20 eV, which has less individual peak height but a greater total area. The resonance Auger spectra should, if measured with sufficient resolution (and freedom from higher-order light) show many pairs of peaks whose energy would add up to a gap between 65.1 eV and a possible final state of Xe^{2+}. For each individual Xe^+ intermediate state, one "first" peak is formed but may be followed by several "second" peaks showing branching to different states of Xe^{2+}. Comparison of the accurately known energies of the Xe^{2+} states[20] with the electron-energy spectra unfortunately does not allow any convincing identification of such pairs because of congestion of the spectra. The PEPECO technique, on the other hand, when brought to a higher level of electron-energy resolution, would evidently solve this problem directly.

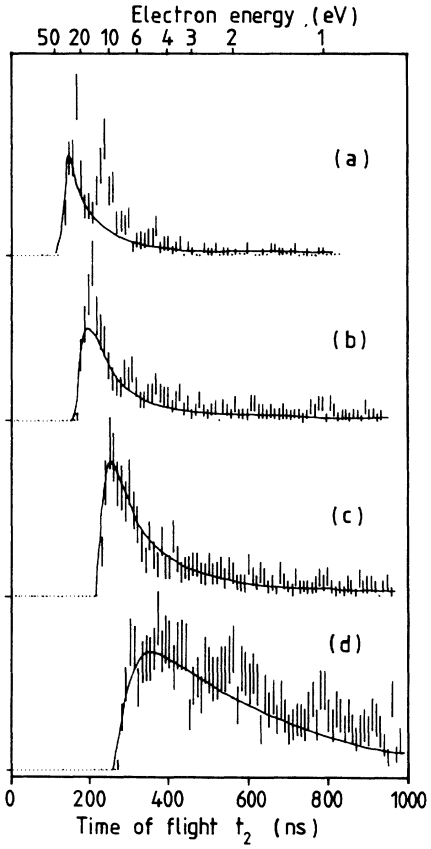

FIG. 6. Electron-energy (long analyzer) derived from the data of Fig. 4 for different energy sums E_1+E_2: (a) 30 ± 5 eV corresponding to the $5s^25p^4$ configuration of Xe^{2+}, (b) 18 ± 4 eV representing mainly $5s5p^5$ final states, (c) 11 ± 2 eV for the shakeup states, (d) 52 eV for $5s^05p^6$. Solid lines drawn on each spectrum are calculated time-of flight spectra for flat electron-energy distributions.

The second two spectra in Figs. 6(c) and 6(d), corresponding to formation of the higher excited states of Xe^{2+}, show little sign of peaks and indeed accurately match the spectra expected on the basis of equal partition of the available energy between two departing electrons. These are clearly the main origin of the continuous distribution seen in the electron spectra and emphasized by Becker *et al.*[2]

More detailed analysis of the data is possible; for instance, distinctly different spectra like those of Fig. 6 are obtained for total energies matching the individual final states ^3P, ^1D, and ^1S of Xe^{2+}. Nevertheless, we feel that the quality of the present data does not justify more detailed dissection, especially as significant improvements to the technique can be foreseen.

DISCUSSION AND PROSPECTS

The major observations of this work are that in the decay of the $4d^95s^25p^6(^2D_{5/2})6p$ resonance of Xe at 65.11 eV, many of the accessible states of Xe^{2+} are populated. Secondly, double Auger processes leading to the ground and first excited configurations of Xe^{2+} occur partly or mainly by autoionizations of intermediate Xe^+ states, whereas the processes leading to higher excited states of Xe^{2+} are almost wholly direct. This information is closely related to the current debate on the dynamics of direct double ionization below inner-shell thresholds[21] where both direct and indirect processes are now known to occur.[12,13] The distinction in behavior between low- and high-energy final Xe^{2+} states must be partially accounted for by the distribution of suitable Xe^+ states; more such states are inevitably available for formation of low-lying states of Xe^{2+}, simply because of the greater available energy range. Other factors affecting direct double-electron ejection might presumably be the phase-space available and the wave-function symmetry, just as in the extended Wannier treatment of two-electron loss in photon or electron impact near threshold.[22,23] Since the symmetry of the initial resonance is $^1P^o$, it ought to follow that direct processes would branch preferentially to $^3P^e$ among the $5s^25p^4$ states of Xe^{2+}, and to $^1P^o$ from the $5s5p^5$ configuration. The other states from these configurations and the configuration $5s^05p^6\ldots$ $^1S^e$ should be "kinetically disfavored," because no electron pair wave function without a node at the Wannier point can be emitted from a $^1P^o$ state in forming them. Even from the present data it is clear that these predictions are not upheld. Just as in the 40.8-eV double photoionization of Xe (Ref. 12) all energetically accessible states seem to be populated with comparable probability, even by ionizations giving a continuous electron distribution. There is hitherto no theoretical explanation of these observations even for the low-energy region. It is questionable whether the decay of the present resonance, 32 eV above the Xe^{2+} ground state could conceivably be considered as within the "threshold region" where the Wannier theory applies. On the other hand, the flatness of the emitted electron-

energy distribution, as seen both in these experiments (Fig. 6) and in previous electron spectra (Becker *et al.*[2]), accords better with near-threshold behavior than with the high-energy behavior exemplified by the x-ray ionization of neon.[24] It may be that flatness of the electron distribution persists to higher energy than other aspects of threshold behavior.

Details of the pathways by which each individual state is populated would be revealed by a higher quality PEPECO spectrum. First priorities for improvement are to obtain better statistics by using a more intense light source and to improve resolution by lengthening the short analyzer and decreasing the time-bin size in data gathering. The experiment was originally intended to be a probe of double-ionization dynamics below inner-shell threshold, and in that region, where electron energies are lower, even a modest improvement in resolution would allow it to reveal hitherto unknown spectra of doubly charged molecular ions, and also the dynamics of their formation. Other two-electron processes such as the normal Auger effect and double ejection from solids[14] can also be studied with great profit by this new technique, and we expect it to be more widely used in the future.

ACKNOWLEDGMENTS

We should especially like to thank the staff of UVSOR who contributed a great deal to the execution of this project. One us (J.H.D.E) gratefully acknowledges support from IMS, which made the project possible.

*Present and permanent address: Physical Chemistry Laboratory, South Parks Road, Oxford OX1 3QZ, United Kingdom.

[1]H. Aksela, S. Aksela, G. M. Bancroft, K. H. Tan, and H. Pulkkinen, Phys. Rev. A **33**, 3867 (1986).

[2]U. Becker, T. Prescher, E. Schmidt, B. Sonntag, and H.-E. Wetzel, Phys. Rev. A **33**, 3891 (1986).

[3]S. Southworth, U. Becker, C. M. Truansdale, P. H. Kobrin, D. W. Lindle, S. Owaki, and D. A. Shirley, Phys. Rev. A **28**, 261 (1983).

[4]V. Schmidt, S. Krummacher, F. Wuilleumier, and P. Dhez, Phys. Rev. A **24**, 1803 (1981).

[5]V. Schmidt, Appl. Opt. **19**, 4080 (1980).

[6]P. A. Heimann, D. W. Lindle, T. A. Ferret, S. H. Liu, L. J. Medhurst, M. N. Piancastelli, D. A. Shirley, U. Becker, H. G. Kerkhoff, B. Langer, D. Szostak, and R. Wehlitz, J. Phys. B **20**, 5005 (1987).

[7]T. A. Carlson, D. R. Mullins, C. E. Beall, B. W. Yates, J. W. Taylor, D. W. Lindle, B. P. Pullen, and F. A. Grimm, Phys. Rev. A **39**, 1170 (1989); T. A. Carlson, W. E. Hunt, and M. O. Krause, Phys. Rev. **151**, 41 (1966); M. O. Krause, J. Phys. (Paris) Colloq. **32**, C4-67 (1971).

[8]T. Hayaishi, Y. Morioka, Y. Kageyama, M. Watanabe, I. H. Suzuki, A. Mikuni, G. Isoyama, S. Asaoka, and M. Nakamura, J. Phys. B **17**, 3511 (1984).

[9]J. H. D. Eland, F. S. Wort, P. Lablanquie, and I. Nenner, Z. Phys. D **4**, 31 (1986).

[10]E. T. Verkhovtseva, E. V. Gnatchenko, P. S. Pogrebnyak, and A. A. Tkachenko, J. Phys. B **19**, 2092 (1986).

[11]I. P. Grant, B. J. McKenzie, P. H. Norrington, D. F. Mayers, and N. C. Pyper, Comput. Phys. Commun. **21**, 2007 (1980); **21**, 233 (1980).

[12]S. D. Price and J. H. D. Eland, J. Phys. B **22**, L153 (1989).

[13]S. D. Price and J. H. D. Eland, J. Electron Spectrosc. Relat. Phenom. (to be published).

[14]H. W. Biester, M. J. Besnard, G. Dujardin, L. Hellner, and E. E. Koch, Phys. Rev. Lett. **59**, 1277 (1987).

[15]H. Yonehara, T. Kasuga, O. Matsudo, T. Kinoshita, M. Hasumoto, J. Yamazaki, T. Kato, and T. Yamakawa, IEEE Trans. Nucl. Sci. **NS-32**, 3412 (1985).

[16]E. Ishiguro, M. Suzui, J. Yamazaki, E. Nakamura, K. Sakai, O. Matsudo, N. Mizutani, K. Fukui, and M. Watanabe, Rev. Sci. Instrum. **60**, 2105 (1989).

[17]P. Kruit and F. H. Read, J. Phys. E **16**, 313 (1983).

[18]Tandem Multichannel plate MCP F1551 (Hamamatsu).

[19]R. Dutil and P. Marmet, Int. J. Mass Spectrom. Ion. Phys. **35**, 371 (1980).

[20]J. E. Hansen and W. Persson, Phys. Rev. A **18**, 1459 (1978).

[21]H. Kossmann, V. Schmidt, and T. Anderson, Phys. Rev. **60**, 1266 (1988).

[22]G. H. Wannier, Phys. Rev. **90**, 817 (1953).

[23]F. H. Read, in *Electron Impact Ionisation,* edited by T. D. Märk and G. H. Dunn (Springer, Vienna, 1985), Chap. 3.

[24]T. N. Chang and R. T. Poe, Phys. Rev. A **12**, 1432 (1975).